Antenna Configurations for the ALMA

Min S. Yun
Last changed 2000-12-11

Revision History:
11/11/98: Added summary and milestone tables. Added chapter number to section numbers, tables and figures (Tamara T. Helfer & M.A. Holdaway).
3/30/00: Updated for the ALMA specifications and added sections describing the zoom spiral configuration concept (Min S. Yun).

Summary

Design concepts and sample layouts for antenna configurations for the ALMA are presented.

Table 15.1 Guidelines for Configuration Design

Main D&D Task	Design a set of configurations which allow for a range of angular resolution and sensitivity
Flexible design philosophy	Configurations must allow for graceful expansion through possible collaboration
Costing	Optimize for shared stations to minimize cost
Site placement	Choose specific locations for antenna placement on Chajnantor site

15.1 Number and Size of Antenna Elements

We assume that the ALMA will comprise N = 64 antennas of 12 m diameter. The geometric collecting area is then 7240 sq. m. The ``collecting length'' nD, the appropriate measure of the mosaicing sensitivity and for the fraction of occupied cells, is 770 m. The collecting area and collecting length are increased by factors of 3.6 and 2.4, respectively, over the old MMA plan with N = 40 and D = 8 m. We note that the array configuration development plan will need to react to the changes and refinements in the array's concept, particularly with regard to possible collaboration with Japanese partners.

15.2 Limiting Configurations, Number of Configurations, and Resolution Scale Factor

15.2.1 Size of the Most Compact Array

The choice of a compact configuration for the ALMA is driven by the desire to maximize surface brightness sensitivity, which is achieved by placing the antennas as close together as is practical.

If we assume a filling factor of 40%, which is a reasonable compromise between the competing requirements of close packing and the resultant maximum acceptable sidelobes, then

the maximum baseline for the compact array is = 150 m.

15.2.2 Size of the Largest Array

The largest configuration is assumed to have a maximum baseline of 3 km. A separate array of 10 km diameter or larger is also being considered.

15.2.3 Number of Configurations and Resolution Scale Factor

Given the assumed sizes of the minimum and maximum arrays, Holdaway (1998a) has performed a cost-benefit analysis for the number of MMA configurations, which showed that the observing efficiency of the MMA would be close to optimal with 4-8 configurations. The calculation appropriate for ALMA produces a similar conclusion (Yun & Kogan 1999). The strawperson configurations consisting of minimum sidelobe donut/double-rings (Kogan 1998) have the resolution scale factor between adjacent configurations of about 2.1, with the outer diameters of 325 m, 680 m, 1430 m, and 3000 m. By sharing the outer ring of antennas as the inner ring of the next larger configuration, the maximum re-use of pads and minimum antenna moves per reconfiguration can be achieved. The most compact array takes advantage of the existing pads in the central compact configuration. The most compact arrays will provide essentially complete sampling of the (u,v) plane in a snapshot observation. The larger arrays will require longer tracks for good imaging and sensitivity.

The main advantage of having configurations with durations longer than a few days (see below) is that there is a greater chance of accomplishing observations with critical weather requirements (such as total power mosaic and high frequency observations) using the full sensitivity of the array. As weather patterns typically persist over several days or even weeks, any "good" observing weather may come in bursts of this time scale. Requiring reconfigurations only on monthly or bi-monthly basis also means that the full complement of 64 antennas are available for most of the observations, unlike for the continuous reconfiguration case.

The minimum and maximum baselines for each array are listed in Table 15.3, along with the size of a sample beam and the time required for the half of the (u,v) cells to be sampled (FOC = 0.5). Note that the shortest baseline does not correspond to the largest angular structure to which the array will be sensitive, as mosaicing with total power data will permit arbitrarily large sources to be imaged.

Table 15.3 Specifications for the ALMA strawperson configurations.

Array	Minimum	Maximum	Array	Time for	Natural
	Baseline	Baseline	Style	FOC = 0.5	Beam at 345 GHz
	[m]	[m]		[hours]	[arcs]
A	30	3000	donut	10	0.050
B	24	1430	donut	2	0.101
C	18	680	donut	0.1	0.22
D	16	325	donut	0.1	0.47
E	16	150	filled	0	0.97

An alternative scheme of a self-similar distribution of pads has also been proposed (Conway 1998, Webster 1998). In such schemes the pad density per unit area falls off as 1/radius squared, and in each configuration the pads over a certain range of radii are occupied. The uv coverages of each configuration are then close to being self-similar, which is useful for projects comparing lines at different frequencies. Because these arrays are continuously self-similar, there is the possibility of accomodating continuous variations in resolution and so these arrays are referred to as 'zoom' arrays. Such schemes also naturally have large pad sharing between configurations. Zoom arrays also naturally give centrally condensed uv coverages, which for the approprate choice of radius over which the pads are occupied in any given configuration (i.e. a factor of about 8) give uv coverages which are close to having a natural Gaussian taper (Conway 1998 and see section 15.3.2.3).

An advantage of zoom arrays is that they can be operated in a highly flexible way. The choice of the number of configurations, resolution step, and the resolutions offered can be left to be decided after construction and can be changed during the lifetime of the array in response to scientific requirements. Depending on the operational constraints, the array may reconfigure continously or in bursts.

The scientific and operational advantages of the continuous reconfiguration mode are further discussed in detail by Conway (1998, 2000a) and by Webster (1998). Observations requiring exact resolution can be better accomodated, and the loss of sensitivity by tapering can be avoided more easily. The total observing efficiency for a continously reconfiguring mode has been argued to be higher than that of a burst mode (Guilloteau 1999, Conway 2000a) although the magnitude of this effect may be small and subject to the type of observations conducted. If only one antenna is moved each day for each transporter, then all antenna reconfigurations may be accomplished within the first few hours of the working day, before high afternoon wind makes moving antennas more difficult.

15.3 Fourier Plane Coverage

15.3.1 Compact Array

The driving considerations for the compact array are maximum surface brightness sensitivity and excellent mosaicing capability. Surface brightness sensitivity is optimized by designing an array with the largest synthesized beam possible, which is achieved by having the shortest baselines possible. The ALMA will be a *homogeneous array*, with total power and interferometric data being collected by the same antennas (Cornwell, Holdaway, & Uson, 1994). Homogeneous array mosaicing image quality is optimized by having a high density of the shortest interferometric baselines and by minimizing the sidelobes in the synthesized beam. Optimizing the short baseline coverage is best achieved with a filled array, which produces a Fourier plane coverage that to first order is a linearly decreasing function of (u,v) distance. The shortest baselines are limited strictly by the minimum safe distance which avoids mechanical collision of the antennas when pointing in arbitrary directions, which depends upon the antenna design, and less strictly by shadowing requirements. Configurations with the highest density of the shortest baselines will be a hexagonal close pack distribution of antennas, which results in a very large grating response in the synthesized beam and is therefore not acceptable. With a minimum distance between antennas of 1.28 D, we can achieve a reasonable sidelobe level of a few percent rms with an array filling factor of 40%. Such a filled compact array will result in complete instantaneous (u,v) coverage, even with only 32 antennas. Some degree of optimization is required, trading off between good short baseline coverage and a large beam on the one hand and minimum synthesized beam sidelobes on the other.

The short spacing requirement for homogeneous array mosaicing, together with the physical inevitability of shadowing, require multiple compact configurations for observations of sources at various declinations. A plan with three compact arrays has been considered (Helfer & Holdaway 1998). The E1 array, with a North-South elongation of 1.2, will cover zenith observations down to somewhat below the onset of shadowing at 50 deg; the E2 and E3 will be progressively more elongated, with elongation of about 1.6 and 3. These three arrays will cover

most of the range of declinations available from the Chajnantor site, -90 deg 53 deg. Observations of the small fraction of the sky which is further north and still visible from Chajnantor will need to be conducted in a hybrid configuration.

The E1 and E2 configurations will utilize a mechanical elevation stop which will limit the elevation to be above 20 deg. This limitation will permit a closer packing of the antennas in the E1 and E2 configurations. While it does remove flexibility from the compact arrays, the E1 and E2 arrays would be largely shadowed below this elevation anyway. The elevation stop will be removed from all or most antennas when they are reconfigured into the E3 array, where the antennas will be sufficiently separated that collisions are no longer a possibility. The general specifications for the E1, E2, and E3 configurations are shown in Table 15.4.

Table 15.4 Specifications for the compact configuration N-S elongations.

Array	Min. N-S	Elev. of first	Min. observing	Max. observing	N-S

	Distance	Shadowing	Elevation	Elevation	Elongation
E1	1.3 D	50 deg	40-45	90	1.2
E2	1.9 D	31 deg	30	50+	1.6
E3	3.0 D	19 deg	14	33+	2.9

An important consideration for having several compact configurations is the cost of building the pads, roads, and cables, though we still need to investigate what these costs are. Overlapping the stations will keep the cost and time involved in reconfiguring the antennas to a minimum. Antenna access is another important consideration: maximize the number of antennas that can be moved by a transporter without moving any other antennas.

15.3.2 Intermediate Arrays

Mosaic observations will also be made in some of the intermediate configurations as the almost complete instantaneous (u,v) coverage and good brightness sensitivity can be achieved with an abundance of short baselines. Quickly increasing atmospheric noise with increasing air mass dictates that it is best to observe a source within a few hours of transit (Holdaway, 1998b), and these configurations should be optimized for short tracks observed within a few hours of transit, over a range of declinations.

The larger array require about 2 hours to achieve complete (u,v) coverage (FOC = 0.5, see Table 15.4), so it should be optimized for somewhat longer tracks, but still within a few hours of transit (Holdaway, 1998b).

The largest array requires up to 10 hours to achieve essentially complete (u,v) coverage. At +/- 5 hours off transit, the sensitivity loss due to the atmosphere will be severe at most frequencies; also, some sources are not above the minimum elevation limit for such long tracks. Nonetheless, the largest array should be optimized for long integrations, keeping in mind that it must also have respectable snapshot coverage for those sources strong enough to be observed in this mode.

As a general requirement, we will want to have some of the shortest baselines (i.e., 16-20 m) present in even the largest arrays to permit single configuration mapping of many wide field objects (Braun, 1993). However, if there is a lot of large structure in the object, multiple configuration imaging may be required. At this point, we do not have a coherent strategy for when to combine data from multiple configurations, nor have we considered the impact of multiple configuration observations on the set of configuration designs. Processing multiple configuration data through a data pipeline may pose an added complexity. Designing in short spacing baselines in all configurations is desirable if it can be accomplished without any serious compromise in overall imaging performance.

Several competing philosophies are currently under consideration for the Fourier plane coverage for the intermediate configurations. One philosophy is to achieve as complete coverage in the Fourier plane as is practical; this approach leads to ring-like arrays, as characterized by Keto

(1997) for snapshot observations and by Holdaway, Foster & Morita (1996) for longer tracks. Donut or double-ring arrays with minimum sidelobes in the synthesized beam, as implemented by Kogan (1997, 1998a), offer many highly desirable characteristics as well. A zoom spiral array proposed by Conway (1998,1999) produces a strongly tapered uv-coverage with continuously changing resolution.

15.3.2.1 Reuleaux Triangles

Keto's Reuleaux triangle configurations, and ring-like configurations in general, yield fairly uniform (u,v) coverage plus a narrow peak at small spatial frequencies. They also offer the advantage of achieving the maximal sensitivity for the longest baselines, resulting in smaller naturally weighted resolution than other types of arrays with the same maximum baseline, which is an attractive characteristic. However, true uniform coverage in the Fourier plane has disadvantages as well:

- the sharp cutoff in (u,v) sampling at large spatial frequencies results in large (10-15%) sidelobes close to the central lobe of the synthesized beam (Holdaway 1997), which may complicate an image deconvolution and thereby lower its dynamic range (Holdaway 1996).

- optimization techniques like the elastic net method used by Keto have so far tended to produce large diameters for the central hole in the Fourier plane coverage. It is probable that this problem can be alleviated to some extent, either by using nested rings or Releaux triangles, or by changing the optimization conditions to include some number of short baselines. The nested triangle approach destroys the uniform Fourier plane coverage.

- unpublished simulations by Morita and by Holdaway show that the excess short spacing coverage which a ring array provides is actually more responsible for high dynamic range in wide-field reconstructions than the uniform Fourier plane coverage.

Webster (1998) has investigated the idea of using nested rings or nested Reuleaux triangles to achieve a compromise between uniform (u,v) coverage and sensitivity to extended structure.

15.3.2.2 Minimum Sidelobe Donut/Double-Ring Concept

Kogan's algorithm produces antenna configurations which minimize the maximum sidelobe levels of the point spread function in some region of the image plane. This approach has the advantage of producing PSFs which should introduce fewer problems in image deconvolution. Kogan has also pointed out that in general, sidelobes that are close to the peak of the PSF can be alleviated using a moderate taper (at the expense of small loss in sensitivity). Another attractive feature of Kogan's approach is that it naturally shrinks the hole in the center of the (u,v) plane as the optimization extends over larger and larger regions in the image plane. This produces good coverage at short baselines in the (u,v) plane, which is one of the main shortcomings of the uniform (u,v) coverage optimization described above.

Kogan's code is flexible and can accept a variety of topographical constraints as inputs. Kogan has investigated arrays with the antennas distributed within an annulus with a fixed outer radius and with varying inner radii. Such a ``donut'' configuration can achieve a significantly more tapered beam (1/r distribution of visibility density) than a single ring configuration, thereby

reducing its near-in sidelobes. The configurations can be designed with maximum pad sharing so that each reconfiguration requires moving only 32 antennas. This added dimension is responsible for the decrease in the scaling factor from 4 to 2.1 compared with the MMA strawperson ring configurations discussed by Helfer & Holdaway (1998) -- see Table 15.3. Another natural advantage of the donut configuration is that hybrid configurations with a N-S elongations of 2 and 3 are naturally achieved during the reconfiguration, and fewer still antennas need to be moved during each reconfiguration if such an intermediate hybrid configuration is needed.

The Kogan arrays are optimized for a snapshot in the zenith direction only; however, changing the declination should change only the positions and not the amplitudes of the sidelobes for a snapshot observation (Kogan 1998a). Preliminary tests suggest that these donut/double-ring arrays are robust against random removal of some fraction (e.g. 10%) of antennas. The earth rotation synthesis tends to fill the gaps in the uv-coverage, suppressing the far sidelobes.

One possible disadvantage to Kogan's approach of minimizing the maximum sidelobe within some region of the points spread function is that rather large sidelobes can lurk just outside the region of optimization. Extending the region of optimization to the full width of the primary beam and applying a weighting function which emphasizes the minimization of the close in sidelobes may be desirable.

We plan to study the ramifications of these competing philosophies and ultimately to select a design based on imaging simulations of sources of different size and structure.

15.3.2.3 Zoom Spirals and Gaussian uv Coverage

Conway (1998) has described a three-armed logarithmic 'zoom' spiral array which is self-similar and allows the possibility of having continuously variable resolution. The most recent version of this array is described by Conway (2000a), in which the spiral arm pitch angle gradually changes so the spiral array becomes a ring in its largest configuration, giving close to uniform uv coverage. The largest 3km configuration therefore has the desirable property that it gives close to the maximum resolution from a given limited 3km diamter area. In contrast for smaller configurations the zoom spiral gives a centrally condensed uv coverage, similar in uv density versus radius to the VLA, but not as extreme. It has been argued that such centrally condensed uv coverages may have significant advantages with respect to imaging quality, and optimising all configurations except the largest for such condensed uv-coverages rather than resolution has been proposed (Conway 2000b). Note that the maximum baseline length is twice as large compared to that for a ring array having the same resolution.

Not only do zoom spirals give centrally condensed uv coverages but for appropriate choices of design parameters the uv point density falls off with radius in a manner very close to Gaussian (Conway 1998). The central part of the zenith snapshot beam then has an almost Gaussian shape and near-in sidelobes are minimized. Conway (2000b) has argued that the resulting arrays with minimized near-in sidelobes give better imaging performance than those which have been optimised to reduce far-out sidelobes. For a uv coverage with a natural Gaussian taper the natural beam is also close to the conventional gaussian restoring beam. This opens up the possibility that narrow-field low dynamic range images can be made without deconvolution (i.e. 'Dirty Imaging') although achieving a high dynamic range will ultimately require some form of deconvolution.

Naturally gaussian tapered uv coverages can be considered as having a well sampled core plus outlier points which help constraining the visibilty extrapolation at higher spatial scales. Sparcer uv coverage in the outer radii would require some interpolation in uv space, however. More uniformly filled coverages require less interpolation over the entire sampled region, but some extrapolation beyond the sampled radius may be needed for support during the deconvolution. For more complex images both uv extrapolation and interpolation become more difficult, and simulations involving a large variety of test images may be needed to determine which of these errors are more important in achieving a good imaging performance.

15.4 Sample Configurations

Since the configuration optimization is still in progress, we do not attempt to present optimized configurations in this document. However, to give the reader a feel for the arrays that the Keto and Kogan algorithms produce, we present sample configurations in Figures 15.1 through 15.6.

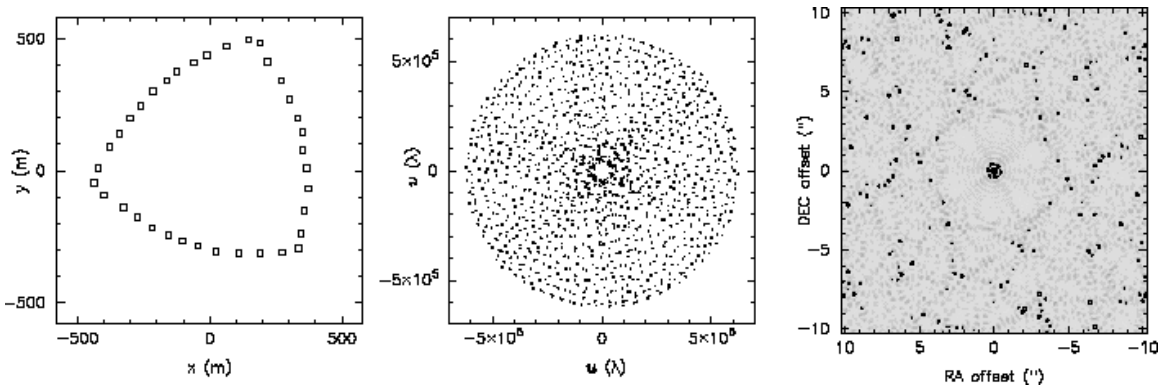

Figure 15.1: Sample Keto array snapshot at 230 GHz. (*left*) Antenna locations in meters, (*middle*) snapshot (u,v) coverage, and (*right*) the resulting synthesized beam, with contours are at 10, 20, 40, 60, 80, 100%. Note the large inner sidelobes.

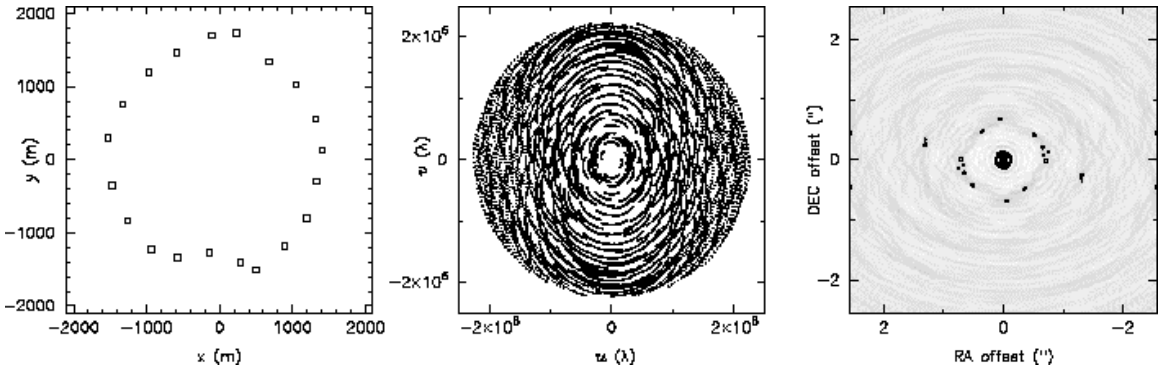

Figure 15.2: Sample 3 km array track for a Keto 20-element array optimized for 4-hour tracks (Holdaway, Foster, & Morita 1996), at 230 GHz. The contours are 0.05, 0.10, 0.15, 0.20, 0.40, 0.60, 0.80, 1.0. The outer sidelobes are reduced for long tracks, but the inner sidelobes remain high.

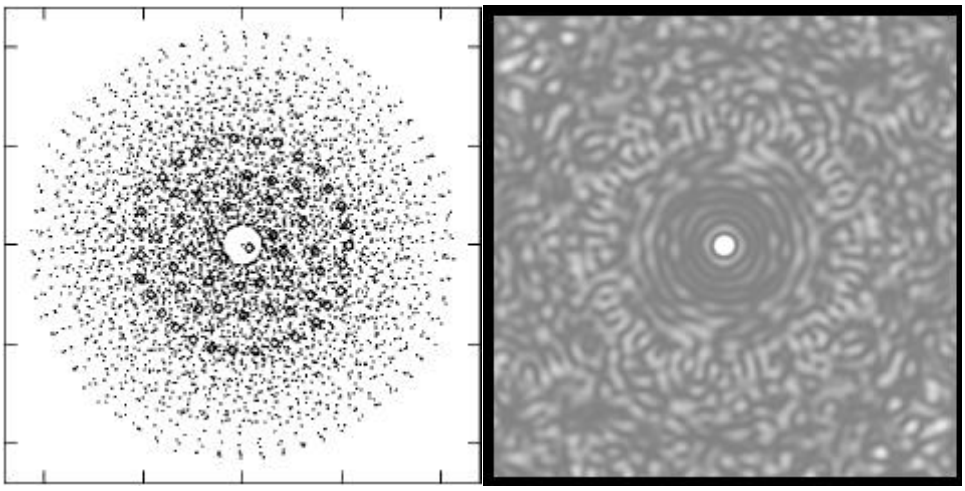

Figure 15.3: Sample compact array pad positions are plotted in diamonds on the left panel along with the zenith snapshot uv coverage. The resulting naturally weighted dirty beam is shown on the right. The greyscale is between -0.05 and +0.10, and the largest sidelobe inside the primary beam is about 5%.

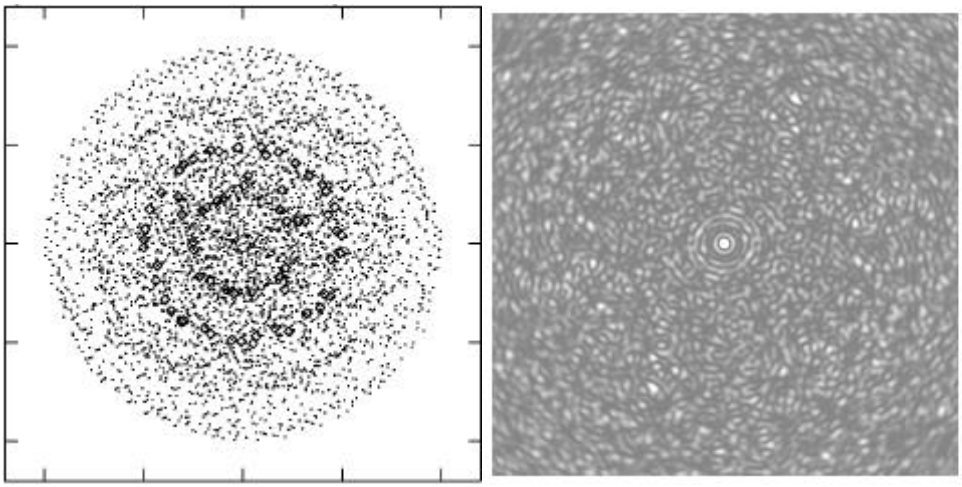

Figure 15.4: Sample Kogan 3 km array pad positions are plotted in diamonds on the left panel along with the zenith snapshot uv coverage. The resulting naturally weighted dirty beam is shown on the right. The greyscale is between -0.05 and +0.10, and the largest sidelobe inside the primary beam is about 10%.

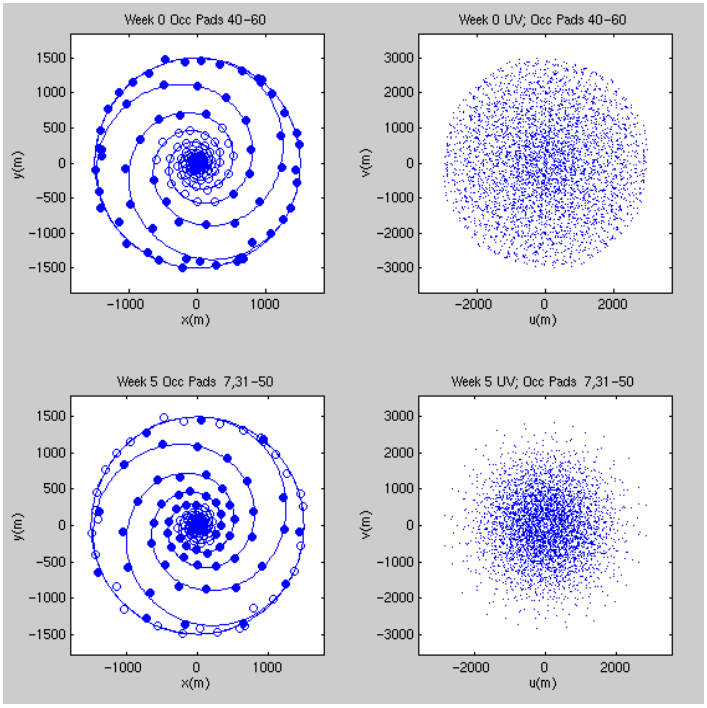

Figure 15.5: The array and zenith uv coverage for the 'zoom spiral' array concept proposed by Conway (1998 and 2000a). Open circles are unoccupied pads and filled symbols are antennas. The top row shows the largest configuration, most antennas lie on the outer ring and so the resolution is maximized. The bottom row shows the array and uv coverage after moving inward approximately half of the antennas. The uv coverage is now centrally condensed and close to gaussian distributed. The resolution is about a factor of 2 less than in the largest configuration. For a 5 month cycle time this array would be reached at week 5.

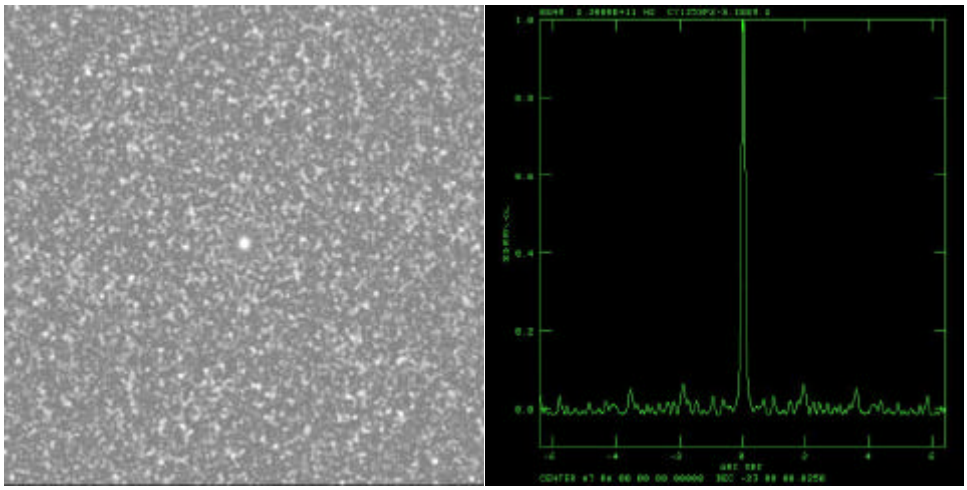

Figure 15.6: Dirty Beam plots for zoom spirals (see Conway 2000b), for zenith snapshot (left) and the N-S slice through the resulting dirty beam (right). The grayscale is between -0.05 and +0.10.

15.5 Hybrid Arrays and Optimal N-S Elongation

From a study of the deviation of synthesized beams from circular as a function of source declination, Foster (1994) concluded that the optimal North-South elongation for tracks of varying length was in the range 1.1-1.3. In order to optimize the elongation of all of the arrays, it is important to know the expected source distribution with declination. Holdaway et al. (1996) assumed a model source distribution in order to estimate the pointing errors for the MMA antenna design. We are now in the process of looking at IRAS source distribution with declination in order to get a better estimate of this function.

Hybrid arrays, made by using stations in adjacent configurations, can be used to help minimize the shadowing and to achieve more circular beams for low-elevation sources. As stated above, a set of hybrid arrays is absolutely required for the compact configurations, but not so crucial for the larger arrays. Hybrid arrays will be studied more in the future when the basic arrays are better determined.

15.6 Topographical Constraints

All of the arrays need to be compatible with the topographic limitations of the Chajnantor site. The basic constraints of the site topography have already been implemented in both the Keto and Kogan algorithms. Digital elevation models (DEMs) of the entire science reserve is now available, and digital topological masks are now being developed (e.g. Butler et al., in preparation).

Radially symmetric configuration designs such as the zoom spiral array or donut/double-ring arrays are intrinsically more susceptible to the topographical constraints, and their implementation may be costly. Preliminary attempts to fit both types of arrays into the topographical constraints are promising (Conway 2000c, Kogan 2000). Development of a cost-mask is highly desirable.

15.7 Interfaces With Other Parts of the ALMA Project

- Antenna: minimum distance for close packing, hard elevation stops
- Antenna: transporter issues, such as intervening antenna clearance, road grade, etc.
- Site Development and Antenna: Antenna Pad Design.
- Site Development: Road Design.
- Local Oscillator/System: underground cables, subarrays for post-move calibrations.

15.8 Other issues to be addressed

There are other issues which have not been examined in this document which deserve closer attention. For example, the arrays need to be optimized for different source declinations, or simultaneously for multiple declinations. Other issues that require further considerations include the effect of earth rotation synthesis (versus snapshots), random losses of antennas, and multi-configuration observations.

Operational concerns such as the frequency and the mode of reconfiguration have also received much attention lately (e.g. Guilloteau 1999, Radford 1999, Yun 1999, Conway 2000). While the ongoing configuration design studies are mostly concerned with the scientific and imaging requirements, weighing the practical concerns such as the cost and maximizing the observing efficiency will ultimately be included in the evaluation process.

References

Braun, R., 1993, ``Telescope Placement at the VLA for Better Single Configuration Imaging", VLA Scientific Memo 165.

Conway, J., 1998, ``Self-Similar Spiral Geometries for the LSA/MMA", MMA Memo #216.

Conway, J., 1999, ``A Comparison of Zoom Arrays with Circular and Spiral Symmetry", MMA Memo #260.

Conway, J., 2000a, ``Observing Efficiency of a Strawperson Zoom Array", MMA Memo #283.

Conway, J., 2000b, ``First Simulations of Imaging Performance of a Spiral Zoom Array; Comparisons with a Single Ring Array", MMA Memo #291.

Conway, J., 2000c, ``A Possible Layout for a Spiral Zoom Array Incorporating Terrain Constraints", MMA Memo #292.

Cornwell, Holdaway, and Uson, 1994, ``Radio-interferometric imaging of very large objects: implications for array design", A&A 271, 697-713.

Foster, S.M. 1994, ``The Optimum Elongation of the MMA A Configuration", MMA Memo #119

Guilloteau, S. 1999, ``Reconfiguring the ALMA Array", MMA Memo #274

Holdaway, M.A., 1998a, ``Cost-Benefit Analysis for the Number of MMA Configurations", MMA Memo #199

Holdaway, M.A., 1998b, ``Hour Angle Ranges for Configuration Optimization", MMA Memo #201

Holdaway, M.A., 1997, ``Comments on Minimum Sidelobe Configurations", MMA Memo #172

Holdaway, M.A., 1996, ``What Fourier Plane Coverage is Right for the MMA?", MMA Memo #156

Holdaway, M.A., Foster, S.M., Emerson, D., Cheng, J., & Schwab, F. 1996, ``Wind Velocities at the Chajnantor and Mauna Kea Sites and the Effect on MMA Pointing", MMA Memo # 159

Holdaway, M.A., Foster, S.M., & Morita, K.-I. 1996, ``Fitting a 12 km Configuration on the Chajnantor Site", MMA Memo #153

Keto, E. 1997, ``The Shape of Cross-correlation Interferometers", ApJ, 475, 843

Kogan, L. 1997, ``Optimization of an Array Configuration Minimizing Side Lobes", MMA Memo # 171

Kogan, L. 1998a, ``Opimization of an Array Configuration with a Topography Constraint", MMA Memo #202

Kogan, L. 1998b, ``Opimization of an Array Configuration with a Donut Constraint", MMA Memo #212

Kogan, L. 1998c, ``A, B, C, and D Configurations in the Shape of Concentric Circles", MMA Memo #217.

Kogan, L. 1999, ``The Imaging Characteristics of an Array with Minimum Side Lobes", MMA Memo #247.

Kogan, L. 2000, ``Fitting of the Largest Configuration (10 km) into the Terrain at the Chajnantor Site", MMA Memo #296.

Radford, S. 1999, ``Antenna Transport Times and Reconfiguration Schedule", MMA Memo #280.

Webster, A. 1998, ``Hybrid Arrays: The Design of Reconfigurable Aperture-Synthesis Interferometers", MMA Memo #214.

Webster, A. 1999, ``Hybrid Arrays: I. The Inner and Outer Hybrids", MMA Memo #239.

Woody, D. 1999, ``ALMA Configurations with Complete UV Coverage", MMA Memo #270.

Yun, M. 1999, ``Sensitivity Loss vs. Duration of Reconfiguration and ALMA Array Design", MMA Memo #276.

Yun, M. & Kogan, L. 1999, ``Cost-Benefit Analysis of ALMA Configurations", MMA Memo #265.